Heliyon 10 (2024) e35173

Contents lists available at ScienceDirect

Heliyon

journal homepage: www.cell.com/heliyon

Research article

Remediation of lead toxicity with waste-bio materials from aqueous solutions in fixed-bed column using response surface methodology

Aanisa Manzoor Shah [a,b], Inayat Mustafa Khan [b], Zhenjie Du [a,*], Rehana Rasool [b], Raihana Habib Kant [c], Shakeel Mir [d], Tahir A. Sheikh [e], Fehim Jeelani Wani [f], M. Ayoub Bhat [b], Javid A. Bhat [b], M.H. Chesti [b], Mumtaz A. Ganie [b], Yasir Hanif Mir [b], Tsering Dolker [b], Sulaiman Ali Alharbi [g], Tahani Awad Alahmadi [h], Shafeeq Ur Rahman [i,**]

[a] *Farmland Irrigation Research Institute, Chinese Academy of Agricultural Sciences, Xinxiang, 453002, China*
[b] *Division of Soil Science and Agricultural Chemistry, Sher-e-Kashmir University of Agricultural Sciences and Technology-Kashmir, Wadura, 193201, Jammu and Kashmir, India*
[c] *Faculty of Agriculture, Sher-e-Kashmir University of Agricultural Sciences and Technology-Kashmir, Wadura, 193201, Jammu and Kashmir, India*
[d] *Division of Soil Science, Sher-e-Kashmir University of Agricultural Sciences and Technology-Kashmir, Shalimar, 190025, Jammu and Kashmir, India*
[e] *Division of Agronomy, Sher-e-Kashmir University of Agricultural Sciences and Technology-Kashmir, Wadura, 193201, Jammu and Kashmir, India*
[f] *Division of Agricultural Economics and Statistics, Sher-e-Kashmir University of Agricultural Sciences and Technology-Kashmir, Wadura, 193201, Jammu and Kashmir, India*
[g] *Department of Botany and Microbiology, College of Science, King Saud University, Riyadh, 11451, Saudi Arabia*
[h] *Department of Pediatrics, College of Medicine and King Khalid University Hospital, King Saud University, Medical City, PO Box-2925, Riyadh, 11461, Saudi Arabia*
[i] *Water Science and Environmental Engineering Research Center, College of Chemical and Environmental Engineering, Shenzhen University, Shenzhen, 518060, China*

ARTICLE INFO

Keywords:
Waste biomaterials
Human hair
Fixed-bed column
Lead adsorption
Box-behnken design
RSM

ABSTRACT

Heavy metal ions pose significant risks to human health, pelagic, and several other life forms due to perniciousness, tendency to accumulate, and resistance to biodegradation. Waste bio-materials extend a budding alternative as low-cost adsorbent to address the removal of noxious pollutants from wastewater on account of being cost-effective and exhibiting exceptional adsorption capacities. The current exploration was accomplished to gauge the performance of raw and modified human hair concerning lead scavenging in a down-flow fixed bed column. The appraisal of column performance under varying operational parameters encompassing bed height (15–45 cm), influent metal ion concentration (60–140 mg L^{-1}), and a solution flow rate (20–40 mL min^{-1}) was performed by breakthrough curve analysis. The consequences acquired were evaluated using the Yoon Nelson, Thomas, Adam-Bohart, and Bed Depth Service Time (BDST) model. Among these employed models, Bed Depth Service Time (BDST) and Thomas models exhibited the highest R-squared value compared to the Yoon Nelson and Adam-Bohart's model for most cases. In addition, the optimization of lead adsorption was followed using the Box-Behnken

* Corresponding author.
** Corresponding author.
E-mail addresses: duzhenjie@caas.cn (Z. Du), malikshafeeq1559@szu.edu.cn (S. Ur Rahman).

https://doi.org/10.1016/j.heliyon.2024.e35173
Received 13 February 2024; Received in revised form 19 July 2024; Accepted 24 July 2024
Available online 26 July 2024
2405-8440/

design of response surface methodology (RSM). The optimal conditions (desirability-1.00) for achieving a goal of maximum percent removal of lead ions were marked to be a bed height of 42.79 cm, solution flow rate of 20.92 mL $min^{-1,}$ and an initial metal concentration of 139.51 mg L^{-1}. Under these optimized conditions, the percent amputation of lead in a fixed bed was observed to be 82.31 %, while the results of the experiment performed approximately under these optimized conditions revealed a percent removal of 85.05 %, reflecting a reasonable conformity with values acquired through Box-Behnken design.

1. Introduction

Water security-the competence mark of a society to ensure the sustainable accessibility of ample water resources that comply quality standards is already under threat and the challenges are projected to intensify in the upcoming epoch [1]. The scarcity of fresh water is an escalating strain in the present era, with a count of approximately 7.7 billion populations. By the year 2050, when the global population is estimated to arrive at 9.4–10.2 billion, representing an escalation of 22–34 %, the issue is projected to become even more pronounced [2]. In accordance with the findings of the United Nations Wastewater Development Report (UNWDR), a staggering amount of approximately 3857.3 trillion cubic meters of freshwater is consumed each year. Within this vast quantity, agriculture accounts for approximately 44 % of water usage, primarily through irrigation and evaporation. Out of the total water consumption, the leftover 56 % is released as wastewater, encompassing a substantial volume of 628 and 314 trillion cubic meters of industrial and municipal wastewater, respectively [3]. Concerning wastewater management, UN Water reported that, by and large, affluent nations effectively address around 70 % of their generated effluent [4]. However, the quotient of wastewater treatment declines to 38 % in upper fairly developed countries, with a further drop of 28 % in developing nations. In countries possessing limited financial resources, wastewater treatment is only possible for a mere 8 %, owing to the heightened costs affiliated with the process. This paucity of treatment leads to detrimental consequences such as greenhouse gas emissions, health risks, and environmental degradation [5].

Heavy metals, pesticides, hydrocarbons, nitrogenous compounds, pharmaceutical residues, phosphorus, and detergents constitute wastewater's most prevalent chemical pollutants. Heavy metal pollution is a subject of apprehension due to its persistent nature, potential toxicity, biodegradation resistance, and ability to accumulate in human organs through the food chain. The occurrence of lead in the human body above the permissible limit is known to disrupt the usual performance of the nervous system, liver, and kidneys [6]. To ensure safety, the acceptable concentration of lead (Pb) ions in potable and surface water is strictly regulated to be below 0.015 mg L^{-1} [7]. For lead discharge, the IS limit in inland surface water is 0.1 mg l-1 [8]. According to the IHME's estimation in 2019, lead exposure was found to be accountable for a significant portion of global health issues. Specifically, it accounted for 62.5 % of instances of idiopathic mental retardation, 8.2 percent of heart diseases related to hypertension, 7.2 % of worldwide occurrences of coronary artery disease, and 5.65 % of strokes [9]. Considering this, it is crucial to prioritize wastewater treatment and effectively address the issue of heavy metal pollution so as to keep these ill imprints at bay.

Recently, the inception of advanced technical interventions has alleviated the proficient elimination of noxious pollutants with the inclusion of heavy metals as well as radionuclide wastes from wastewater [10]. These interventions encircle ultra-filtration, coagulation, solvent extraction, precipitation, membrane filtration, neutralization, electro-dialysis, reverse osmosis, and ion exchange, and the effectiveness of these techniques in addressing the remediation of heavy metals has been well documented and proven successful [11]. Although these technologies showcase efficiency, they do face certain limitations, such as elevated operational costs, extensive instrumentation, and primary suitability for small-scale water treatment applications. The adsorption method has emerged as an exceptional remediation technique and is widely embraced as a water treatment technique due to its economic efficiency, seamless operation, and the advantage of not requiring bulky instrumentation. This methodology offers the significant advantage of removing heavy metals from water and allows for the recovery and reusability of spent adsorbents. Consequently, these interventions strengthen the waste-to-wealth approaches, promoting sustainable and resourceful practices.

Waste bio-materials frame a budding alternative as low-cost adsorbents with regard to heavy metal remediation of wastewater on account of being cost-effective and exhibiting exceptional adsorption capacities [12]. Being an abundant and inexpensive biological resource, keratin biomaterials have the potential to be employed as economically efficient and abundant resources for the remediation of heavy metals, making them promising bio-sorbents [13]. A wide array of such materials encircling feather, hair, wool, and horn have been employed as proficient bio-sorbents, either as such or after activation for heavy metal removal, owing to the elevated contents of hydroxyl, amino, carboxyl, and sulfur-containing functional groups [14]. Human hair is often regarded as waste and is disposed of through incineration or finds its fate in landfills, with only a meager portion being recycled and cast off as biodegradable surfactants or fertilizers [15]. The hair fiber contains proteins called keratins and keratin-associated proteins, which play a significant part in the development of hair fibers. Keratin is a captivating protein and a potential attractant of metal ions. Paying to a profound cysteine content, keratin has the proficiency to form disulfide bonds and crosslinks. This characteristic contributes to the strong mechanical properties of human hair and its low solubility in water [16]. However, engineering the characteristics of an adsorbent is a feasible approach to tune the metal adsorption. To address this, modifications through oxidation or reduction reactions are utilized to cleave the disulfide interactions in human hair, forming cysteic acid residues. This process enhances the hydrophilic features of hair, thereby improving its ability to adhere to metal ions that are positively charged [17]. Nevertheless, the adsorption process using these adsorbents is influenced by several operational parameters, and it is crucial to optimize their effects and interactions to enhance process efficiency.

Exploring the optimal level through classical and conventional approaches can be time-consuming, often demanding ample time and many experiments [18]. Through the integration of a statistical model, the remarkable feat of forecasting the combined imprints of different factors on adsorption efficiency, ultimately leading to optimization, has been accomplished [19]. Response Surface Methodology (RSM) is a strategic approach in experimental design that helps reduce the number of experiments needed. It allows us to optimize the desired response within a given range by systematically identifying the most suitable conditions [20]. This optimization is crucial to maximize the effectiveness and proficiency of the adsorption approach while minimizing the cost at the scale-up phase [21]. Adhering to the attributes mentioned above, the conduct of this investigation was to devise experiments to develop empirical models, followed by the appraisal of optimum operating conditions for the operational parameters (bed height, initial metal ion concentration, and solution flow rate) to achieve the peak response (lead adsorption) onto modified human hair using response surface methodology.

2. Experimental procedure

2.1. Materials

The human hair left-over mixture (only male folk aged 13–35) was procured from a local barbershop. The sample was cleansed using commercial detergent to prepare the adsorbent and then thoroughly rinsed with de-ionized water. Subsequently, it was left for drying at room temperature. The dried hair samples were chopped to an approaching length of <5 mm with scissors and kept in air-tight polyethylene bags for subsequent laboratory analysis. The processed human hair was acid and bio-modified to improve its effectiveness as a biosorbent for removing heavy metals.

2.1.1. Acid modification

The processed human hair was treated with 0.1 N HNO_3 in the ratio of 1:20. After a brief soaking period, the agitation of the mixture was performed at 50 °C, employing a thermostatic shaker at 200 rpm for 4 h. Ensuing this, the treated adsorbent was subjected to multiple washings with de-ionized water, followed by drying at room temperature. These dried samples were stored for subsequent laboratory analysis.

2.1.2. Bio-modification

The processed hair samples were mixed with a liquid formulation of wet *Bacillus subtilis* biomass in the ratio of 1:34 and shaken for 72 h in the thermostatic shaker at 27°C and 45 rpm. After being treated, the samples were rinsed with de-ionized water, filtered, and then dehydrated at room temperature. The resulting adsorbent samples were stored using air-tight polyethylene bags for further examination.

2.1.3. Preparation of stock solution

Every chemical employed in the current experiment was of analytical grade without any additional purification steps. To prepare a stock solution of 1000 ppm for lead ions, an appropriate amount of lead nitrate [$Pb(NO_3)_2$] metal salt was dissolved in de-ionized water with subsequent dilution to a volume of 1 L with de-ionized water. The strength of the experimental solution was ascertained by referencing its calibration curve. The calibration curve for Pb (II) was created using six working standard solutions formulated by diluting stock solutions to the requisite strengths. These working standard solutions were used to calibrate the atomic absorption spectrophotometer (AAS), and the resulting plot of absorbance versus Pb (II) ion concentration was used to construct the calibration curve. The sample's lead ion concentration was assessed by measuring its absorbance at 216.9 nm wavelength and employing an atomic absorption spectrophotometer.

2.2. Fixed bed column adsorption

The performance of adsorbents (raw, acid, and bio-modified human hair) was evaluated in a column of downward flow using 24″ length and 4″ diameter PVC pipes. The material packed in the column was supported by glass wool on either side to prevent floatation of adsorbent and avoid outlet clogging during the operation. Synthetic wastewater of lead was delivered down the column at varying flow rates, which were adjusted using specific valves. These experiments were performed at room temperature. The collection of effluent samples from the column outlet was executed at pre-determined time periods. The remnant lead ion concentration quantification in acquired effluent samples was assessed with an atomic absorption spectrophotometer. In addition, the effect of operational parameters encircling bed height (15–45 cm), solution flow rate (20–40 mL min^{-1}), and initial metal concentration (60–140 mg L^{-1}) on lead adsorption were gauged and optimized using response surface methodology.

2.2.1. Analysis of breakthrough curves

The column performance regarding lead adsorption from aqueous solution was analyzed using breakthrough curves. The breakthrough curve refers to a pictorial illustration of the ratios of effluent concentration to inlet concentration charted against elapsed time (C_t/C_o vs. t) or effluent volumes (V) used [22]. A breakthrough curve is imperative in assessing a packed bed's performance in a fixed-bed adsorption system. It offers appreciated information about the shape and timing of the breakthrough, which is instrumental in defining the operational characteristics as well as the dynamic behavior of the adsorption column [23]. In the current study, the breakthrough time was appraised at a C_t/C_o value equivalence of 10 %.

The calculation of effluent volume was performed using equation (1) as:

$$V_{eff} = Q.t \tag{1}$$

Where V_{eff} signifies effluent volume accumulated in mL; Q represents the solution flow rate in mL $min^{-1,}$ while t_{total} is the complete flow time (min).

The quantity of metal adsorbed (in mg) in total by the column was determined by calculating the area underneath the plot of the metal ion concentration employing numerical integration as represented in Equation (2):

$$q = \frac{QA}{1000} = \frac{Q}{1000} \int_{t=0}^{t=total} (C_o - C_t)\, dt \tag{2}$$

Where,

Q represents solution flow rate (mL min^{-1}); C_o illustrates influent concentration (mg L^{-1}); C_t depicts effluent concentration at t time while A represents the area beneath the breakthrough curve commencing from time 0 to time t. The computation of maximum adsorption capacity was accomplished following Equation (3):

$$q_m = \frac{q_{total}}{m} \tag{3}$$

where m denotes the adsorbent amount (g) packed in column.

The total amount of metal ions delivered to column (M_{total}) was computed using equation (4):

$$M_{total} = \frac{C_o\, Qt_{total}}{1000} \tag{4}$$

The percent removal of metal ions was computed in accordance with equation (5):

$$\text{Total Removal } (\%) = \frac{q_{total}}{M_{total}} \times 100 \tag{5}$$

The estimation of the mass transfer zone, MTZ (cm), was worked out as represented in equation (6):

$$MTZ = \left(\frac{t_{total} - t_b}{t_{total}}\right) \times Z \tag{6}$$

where z denotes the bed height (cm).

2.2.2. Modeling of column adsorption

The performance of the fixed-bed column was predicted using different models on account of their regression coefficient (R^2) and the best fit of the straight line. The models employed include the Thomas, Adams–Bohart, Yoon–Nelson, and Bed Depth Service Time models.

1. Thomas model: This model relies on second-order kinetics with the assumption that chemical reactions do not constrain biosorption but rather are governed by interfacial mass transfer [24]. The determination of model parameters is carried out in accordance with the specified mathematical expression of equation (7):

$$\frac{C_t}{C_o} = \frac{1}{1 + exp\left(K_{th}\frac{q_o * m}{W} - K_{th}\, C_o t\right)} \tag{7}$$

   Where K_{th} represents Thomas kinetic coefficient (ml/mg min); W signifies the solution flow rate (mL min^{-1}).
2. Yoon–Nelson model: The undertaking of this model is the rate at which the probability of adsorption decreases for every adsorbate particle is directly proportional to both the likelihood of adsorbate breakthrough on sorbent surface as well as adsorbate adsorption [25]. The mathematical model is illustrated in equation (8) as follows:

$$\frac{C_t}{C_o - C_t} = \exp(K_{YN} t - \tau K_{YN}) \tag{8}$$

   K_{YN} signifies the Yoon-Nelson rate (min^{-1}), and τ signifies the time entailed for 50 % breakthrough (min).
3. Adams–Bohart model: The current model's rationale is that the adsorption rate is directly proportionate to both the adsorption capacity and the left-over concentration. It is specifically designed to pronounce the initial portion of the acquired breakthrough curve [26]. The mathematical representation is specified in equation (9) as follows:

$$\frac{C_t}{C_o} = \exp K_{AB}\, C_o\, t - K_{AB}\, N_o \frac{Z}{F} \tag{9}$$

where C_t illustrates the left over adsorbate concentration as a function of time; K_{AB} illustrates the kinetic constant (1/mg min), N_o mirrors the saturation concentration (mg L^{-1}); Z represents the bed height of the fixed-bed column, and F reflects the superficial velocity (cm min^{-1}).

4. Bed Depth Service Time Model: This model assumes that the adsorption rate is governed by the apparent interaction between the adsorbate and the unutilized adsorbent capacity [27]. equation (10) establishes a linear correlation between the depth of the bed and the duration of service time as:

$$t=\frac{N_o}{C_o u} Z - \frac{1}{KC_o}\ln\left(\frac{C_o}{C_t}-1\right) \tag{10}$$

Where N_o represents the dynamic bed capacity (mg g^{-1}); u denotes the linear flow rate (cm min^{-1}), which is demarcated as the ratio of the volumetric flow rate (cm^3 min^{-1}) to the cross-sectional area of the bed (cm^2). Furthermore, K represents the adsorption rate constant (L mg^{-1} min^{-1}) while C_o and C_t refer to the influent and effluent Pb^{2+} concentration at any time t, respectively.

2.2.3. Optimization of variables by response surface methodology (RSM)

On the grounds of preliminary batch studies, the acid-modified human hair exhibited an edge over raw and bio-modified human hair with regard to lead adsorption. In view of this, only acid-modified human hair was subject to an optimization process using response surface methodology. Three level-three factors of the RSM-based Box-Behnken design were engaged to appraise the individual as well as collaborative imprints of operational parameters on lead adsorption. A total of seventeen experiments were devised (Table 1), with the studied operational parameters as bed height (15–45 cm), solution flow rate (20–40 mL min^{-1}), and initial metal concentration (60–140 mg L^{-1}). The response variable (lead adsorption) was expressed as a function of operating variables using a second-order polynomial model and is represented in equation (11) as:

$$Y=\beta_o+\sum_{i=0}^{k}\beta_i X_i \sum_{i=0}^{k}\beta_{ii} X_i^2+\sum\nolimits_{1\le i\le j}^{k}\beta_{ij}X_iY_j+\varepsilon \tag{11}$$

Where,

Y mirrors the predicted response (Adsorption efficiency), X_i reflects the operating variable, β_o is the constant coefficient, β_i and β_{ii} are the linear and quadratic coefficients of input variables, β_{ij} is the interaction coefficient of X_i and X_j input variables, and ε is the random error. The effectiveness of the mentioned model, the impact of individual parameters, and their combined Influence were assessed by applying an analysis of variance (ANOVA). Fischer's F-test, *p*-value, and lack of fit analysis of the employed model were accomplished by employing Design-Expert software. In addition, response surface plots and standardized effects were generated to elucidate the impact of regulating factors on the response variable and overall value of the model.

2.3. Regeneration and reusability of adsorbents

Desorption experiments were performed for lead ions after the corresponding adsorption step using raw and modified human hair. The reusability analysis was performed onto the previously exhausted column of 45 cm bed height, a solution flow rate of 20 ml min^{-1}, and an initial metal concentration of 140 mg L^{-1} 0.1 mol/L EDTA solution was delivered to the exhausted column in down-flow

Table 1
RSM-based Box-Behnken experiment for Column operational variables with actual and predicted response.

Std.	Run	Factor 1	Factor 2	Factor 3	Actual Response	Predicted Response
		A:Bed Height	B:Flow Rate	C:Initial Concentration	Percent Removal	Percent Removal
17	1	30	30	100	76.59	75.76
14	2	30	30	100	75.32	75.76
9	3	30	20	60	77.52	76.94
10	4	30	40	60	71.56	71.07
12	5	30	40	140	73.13	73.71
11	6	30	20	140	78.91	79.40
3	7	15	40	100	69.31	69.28
15	8	30	30	100	75.01	75.76
6	9	45	30	60	79.23	79.78
13	10	30	30	100	75.98	75.76
1	11	15	20	100	72.89	72.95
5	12	15	30	60	70.09	70.61
8	13	45	30	140	80.77	80.26
16	14	30	30	100	75.92	75.76
7	15	15	30	140	75.77	75.22
4	16	45	40	100	74.34	74.28
2	17	45	20	100	82.14	82.17

direction at a flow rate of 5 ml min^{-1}. The metal ion concentration from the column outlet was quantified with an atomic absorption spectrophotometer. The regenerated column was rinsed with distilled water and subjected to adsorption again. The regeneration efficiency was computed as:

$$\text{Regeneration Efficiency}(\%) = \frac{q_{reg}}{q_{org}}$$

Where q_{reg} represents the adsorption capacity of regenerated adsorbent; q_{org} signifies the adsorption capacity of fresh adsorbent.

3. Results and discussion

3.1. Analysis of column performance

The computed values for column adsorption capacity (q_m), effluent volume (v_{eff}), breakthrough time (t_b), percent removal (%), and extent of mass transfer zone (Z_m) are encapsulated in Table 2. The column sorption capacity of acid-modied human hair was higher in contrast to bio-modified and raw human hair. These observations might be attributed to the nitric acid modification which enhances the oygen containing functional groups of thre adsorbent, thereby enhancing the adsorption capacity of meta ions from aqueous solutions [28]. In addition, the reduction of sulfide bonds in human hair to mercapto groups (-SH) in response to chemical treatment f acilitates the coordination of sulfur atoms with metal ions [29]. The acquired breakthrough curves under varied bed height (a-c), flow rate (d-f), and initial metal ion concentration (g-i), concerning raw, acid, and bio-modified human hair are presented in Fig. 1. During the initial phase, the adsorbents' marked a rapid adsorption of lead, followed by a swift decline in the adsorption rate. The column didn't realize complete exhaustion or saturation over a stipulated time of 150 min; however, relative stability for lead adsorption was marked after approximately 120 min of the time interval. The fluctuations in the profile of breakthrough plots are accounted to the variation of operational parameters and are conferred in succeeding subdivisions.

3.1.1. Influence of bed height

The influence of bed height on lead adsorption in a fixed-bed column was appraised at three distinct bed heights encircling 15 cm, 30 cm, and 45 cm using a solution flow rate of 20 mL min^{-1} and metal ion solution of 60 mg L^{-1} concentration. The results revealed that the breakthrough time increased from 15.04 to 58.88 min, 23.63–68.33 min, and 22.77–68.33 min for raw, acid, and bio-modified human hair, respectively (Table 2; Fig. 1). Consequently, it can be inferred that the smaller the bed height, the faster the attainment of the breakthrough point. The higher bed depth requires extended time for saturation than lower bed depth [30]. In addition, the breakthrough time for acid-modified human hair possessed an edge over raw and bio-modified human hair, reflecting a higher lead uptake by acid-modified human hair. The percent removal of lead ions increased from 67.15 to 79.97 %, 70.83–81.82 %, and 69.33–80.94 % for raw, acid, and bio-modified human hair, respectively, with the surge in column bed height from 15 to 45 cm. The column sorption capacity (q_m) increased from 0.46 to 0.55 mg g^{-1}, 0.59–0.65 mg g^{-1}, and 0.49–0.57 mg g^{-1} for raw, acid, and bio-modified rice straw, with an increase in bed height from 15 to 45 cm. The rise in the lead uptake capacity with increased bed height of the column might be accredited to the prevalence of a greater number of active sites on the adsorbent. This increase in active sites

Table 2
Fixed bed column paramters for lead adsorption.

Adsorbent	Z (cm)	FR (mL min^{-1})	C_o (mg L^{-1})	t_b-10 % (min)	V_{eff} (mL)	q_m (mg g^{-1})	% Removal	Z_m (cm)
HH	15	20	60	15.04	3000	0.46	67.15	13.49
	30	20	60	39.97	3000	0.50	75.77	22.00
	45	20	60	58.88	3000	0.55	79.97	27.33
	45	30	60	24.06	4500	0.42	71.29	37.78
	45	40	60	14.21	6000	0.38	62.96	40.73
	45	20	100	16.33	3000	0.61	80.01	40.10
	45	20	140	14.18	3000	0.63	81.01	40.74
AMHH	15	20	60	23.63	3000	0.59	70.83	12.63
	30	20	60	41.57	3000	0.62	77.52	21.68
	45	20	60	68.33	3000	0.65	81.82	24.50
	45	30	60	38.68	4500	0.50	79.23	33.33
	45	40	60	18.48	6000	0.45	68.99	39.45
	45	20	100	33.25	3000	0.67	82.14	35.02
	45	20	140	15.04	3000	0.69	85.05	40.48
BMHH	15	20	60	22.77	3000	0.49	69.33	12.72
	30	20	60	44.26	3000	0.54	76.25	21.14
	45	20	60	68.33	3000	0.57	80.94	24.50
	45	30	60	36.53	4500	0.48	76.20	34.04
	45	40	60	14.61	6000	0.46	67.37	40.61
	45	20	100	21.48	3000	0.63	81.84	38.55
	45	20	140	14.18	3000	0.66	83.87	40.74

HH-Human Hair AMHH-Acid Modified Human Hair BMHH-Bio-Modified Human Hair Z-bed height FR-flow rate t_b (10 %)-breakthrough time V_{eff}-effluent volume q_m-column sorption capacity Z_m-length of mass transfer zone.

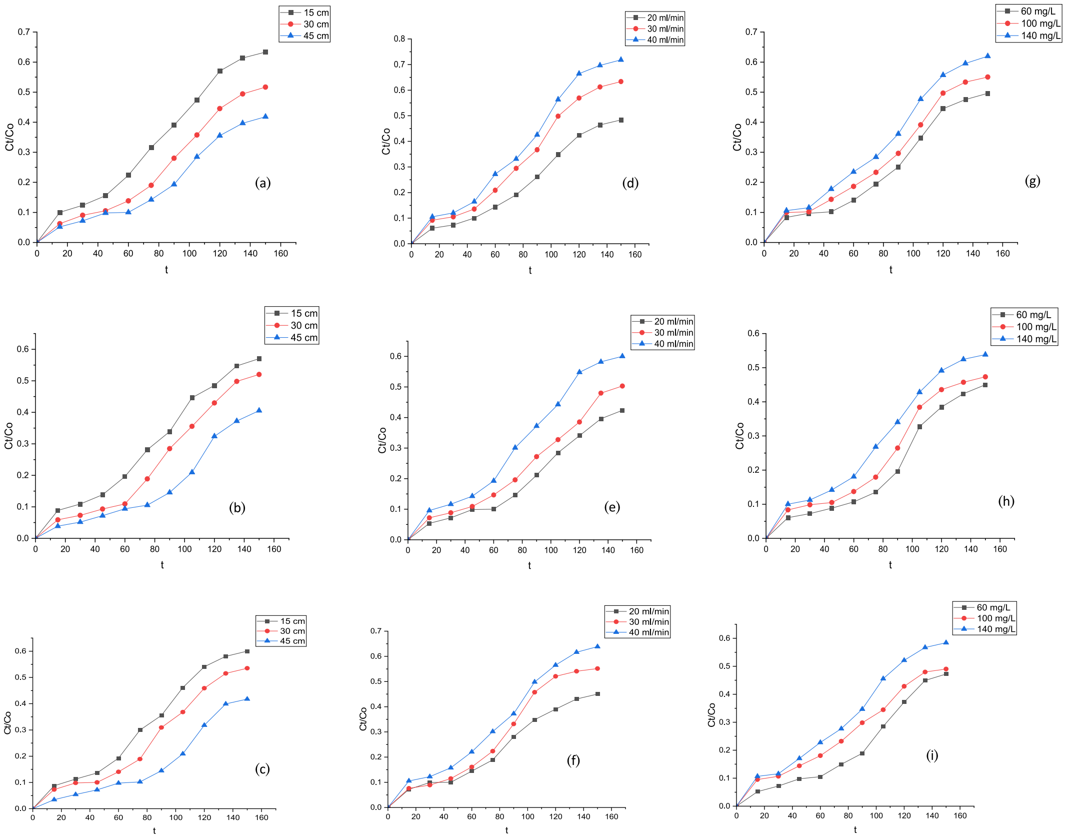

Fig. 1. Breakthrough curves for lead adsorption onto raw (a, d, g), acid (b, e, h) and bio-modified (c, f, i) human hair using various bed heights (a–c), flow rates (d–f) and metal ion concentrations (g–i).

allows for more binding sites, facilitating the course of adsorption [31,32]. Furthermore, the elevated bed height directs to enhanced service interval for breakthrough as well as exhaustion time at a specified concentration. Similar dependence has been put forth by Imran et al. [33] and Shah et al. [34].

3.1.2. Influence of flow rate

To appraise the prominence of various flow rates (20–40 mL min^{-1}) on lead adsorption, a fixed bed column was run at an invariable bed height of 45 cm and an initial metal concentration of 60 mg L^{-1} and the respective breakthrough plots are demonstrated in Fig. 1 (d–f). The breakthrough time, in addition to breakthrough volume, decreased with a rise in solution flow rate. The breakthrough time varied from 58.88 to 14.21 min, 68.33 to 18.48 min, and 68.33 to 14.61 min for raw, acid, and bio-modified human hair, respectively. The lead removal percentage was marked to decrease from 79.97 to 62.96 % for human hair, 81.82 to 68.99 % for acid-modified human hair, and 80.94 to 67.37 % for bio-modified human hair on increasing the flow rate from 20 mL min^{-1} to 40 mL min^{-1}. The column sorption capacity (q_m) marked a drop from 0.55 to 0.38 mg g^{-1}, 0.65 to 0.45 mg g^{-1}, and 0.57 to 0.46 mg g^{-1} for raw, acid, and bio-modified rice straw, with an increase in flow rate from 20 to 40 mL min^{-1}. At elevated solution flow rates, the dwelling span of metal ions in a fixed-bed column declines, leading to a decreased interaction between the adsorbent surface and metal ions [35]. At lower flow rates, the metal adsorption increases steadily, resulting in a delay of adsorbent saturation, while at higher flow rates, the bed saturation is attained rapidly. The attainment of bed saturation at lower flow rates demands an extended contact time. The saturation of sites occurs as the influent flow persists, resulting in decreased proficiency in the removal of metal ions. Eventually, an instant is reached at which the inlet concentration matches the outlet concentration, indicating that the column has become saturated [36].

3.1.3. Influence of initial metal concentration

The track of initial metal ion concentration in relation to lead uptake was appraised at an invariable flow rate of 20 mL min^{-1} and a bed height of 45 cm and the breakthrough curves are illustrated in Figure-1 (g-i). The results elucidated that the breakthrough time declined from 58.88 to 14.18min for human hair, 68.33–15.04 min for acid modified human hair and 68.33 to 14.18 min for bio-modified human hair, while increasing the initial metal ion concentration from 60 to 140 mg L^{-1}. Furthermore, the percent removal of lead ions was marked to increase from 79.97 to 81.01, 81.82–85.05, and 80.94–83.87 %, for raw, acid, and bio-modified human hair, respectively, while increasing the influent metal concentration from 60 to 140 mg L^{-1}. The column sorption capacity (q_m)

increased from 0.38 to 0.63 mg g^{-1}, 0.45–0.69 mg g^{-1}, and 0.46–0.66 mg g^{-1} for raw, acid, and bio-modified rice straw, with an increase in metal ion concentration from 60 to 100 mg L^{-1}. At higher initial metal concentrations, the elevated removal proportion of lead ions might be accredited to both the increased rate of adsorption in hand and the consumption of all accessible binding loci for adsorption. Furthermore, the enhanced uptake of lead ions in response to elevated metal ion concentration might be due to the creation of a stronger propulsion for the transmission process to daze the mass transfer resistance [37]. Typically, with low initial metal ion concentrations, the proportion of metal ions to accessible binding sites on adsorbent is minimal. As a result, the adsorption process becomes less dependent on adsorbent characteristics. Despite this, as the quantity of metal ions escalates, a larger amount of adsorbent is exposed to these adsorbate molecules, which aftermaths results in an enhanced capacity to adsorb metal ions [38].

3.2. Mathematical modeling of column adsorption

The column efficiency can be predicted by exploiting the variables acquired from the breakthrough curves. Four mathematical models employed in this study for predicting column efficiency in hand with its dynamic behavior encompass the Thomas model, Adam Bohart model, Yoon-Nelson model, and Bed Depth Service Time (BDST) model. Parameters computed from the employed models are presented in Table 3. In addition, the parameters for the BDST model were computed at 10 %, 20 %, and 30 % break-through. The higher correlation coefficient (R^2), a value closer to 1, suggested the suitability of all models to anticipate the adsorption accomplishment of fixed-bed columns using raw and modified human hair. The overall picture of models employed elucidated a higher

Table 3
Model Parameters for fixed-bed adsorption of lead under different operating conditions.

Experimental Conditions			Thomas Model								
			Human Hair			Acid-Modified Human Hair			Bio-Modified Human Hair		
Z (cm)	C_o (mg L^{-1})	FR (mL min^{-1})	K_{th} (mL/mg-min)	q_0 (mg/g)	R^2	K_{th} (mL/mg-min)	q_0 (mg/g)	R^2	K_{th} (mL/mg min)	q_0 (mg/g)	R^2
15	60	20	0.145	0.787	0.98	0.172	0.790	0.97	0.134	0.789	0.97
30	60	20	0.140	1.088	0.97	0.145	1.107	0.97	0.140	1.089	0.97
45	60	20	0.131	1.724	0.97	0.129	1.781	0.97	0.130	1.750	0.97
45	60	30	0.139	1.038	0.97	0.140	1.405	0.99	0.140	1.081	0.95
45	60	40	0.143	0.715	0.98	0.145	1.126	0.97	0.132	1.003	0.98
45	100	20	0.132	1.751	0.97	0.130	1.799	0.94	0.131	1.777	0.98
45	140	20	0.135	1.772	0.98	0.132	1.781	0.96	0.133	1.780	0.98

Experimental Conditions			**Yoon-Nelson Model**								
			Human Hair			**Acid-Modified Human Hair**			**Bio-Modified Human Hair**		
Z (cm)	**C_o (mg L^{-1})**	**FR (mL min^{-1})**	**K_{YN} (min^{-1})**	**τ (min)**	**R^2**	**K_{YN} (min^{-1})**	**τ (min)**	**R^2**	**K_{YN} (min^{-1})**	**τ (min)**	**R^2**
15	60	20	0.022	114.375	0.98	0.023	125.508	0.98	0.022	119.847	0.97
30	60	20	0.022	137.337	0.98	0.021	137.026	0.97	0.022	134.630	0.97
45	60	20	0.020	157.925	0.98	0.020	163.541	0.98	0.022	160.695	0.98
45	60	30	0.023	115.213	0.97	0.020	143.199	0.99	0.023	126.438	0.96
45	60	40	0.025	102.254	0.98	0.021	119.760	0.97	0.022	114.357	0.98
45	100	20	0.020	130.957	0.98	0.019	143.982	0.95	0.018	142.289	0.98
45	140	20	0.021	116.863	0.98	0.019	129.291	0.97	0.020	122.181	0.98

Experimental Conditions			**Adam Bohart Model**								
			Raw Human Hair			**Acid-Modified Human Hair**			**Bio-Modified Human Hair**		
Z (cm)	**C_o (mg L^{-1})**	**FR (mL min^{-1})**	**K_{AB} (1/mg-min)**	**N_o (mg L^{-1})**	**R^2**	**K_{AB} (1/mg-min)**	**N_o (mg L^{-1})**	**R^2**	**K_{AB} (1/mg-min)**	**N_o (mg L^{-1})**	**R^2**
15	0 60	20	0.000278	161.864	0.95	0.000304	169.259	0.95	0.000273	163.585	0.95
30	60	20	0.000274	86.678	0.97	0.000301	85.043	0.96	0.000259	86.243	0.96
45	60	20	0.000263	63.034	0.97	0.000291	63.161	0.98	0.000246	62.086	0.98
45	60	30	0.000267	79.608	0.95	0.000295	90.423	0.98	0.000281	82.575	0.95
45	60	40	0.000271	100.701	0.95	0.000304	110.083	0.95	0.000314	108.179	0.96
45	100	20	0.000274	97.630	0.97	0.000296	101.860	0.95	0.000253	104.122	0.97
45	140	20	0.000281	128.612	0.96	0.000302	136.051	0.95	0.000259	132.752	0.96

Experimental Conditions	**BDST Model**								
	Raw Human Hair			**Acid-Modified Human Hair**			**Bio-Modified Human Hair**		
	K (L mg^{-1} min^{-1})	**N_o (mg g^{-1})**	**R^2**	**K (L mg^{-1} min^{-1})**	**N_o (mg g^{-1})**	**R^2**	**K (L mg^{-1} min^{-1})**	**N_o (mg g^{-1})**	**R^2**
$C_t/C_o = 0.1$	1.418	21.641	0.99	1.531	22.065	0.98	1.323	22.090	0.99
$C_t/C_o = 0.2$	0.974	25.894	0.98	0.974	27.876	0.98	0.966	26.876	0.97
$C_t/C_o = 03$	0.178	29.889	0.98	0.030	33.388	0.97	0.037	31.871	0.96

R-squared value for Bed Depth Service Time (BDST) and Thomas model for most cases compared to Yoon Nelson and Adam-Bohart's model. The best fit acquired using the BDST model (R^2: 0.96–0.99) demonstrates a direct correlation between the service span of the fixed-bed column and bed height [39]. The suitability of the Thomas model (R^2: 0.95–0.97) confirms that the lead adsorption follows the second-order kinetics with no axial dispersion [40].

3.2.1. Thomas model

The data presented in Table 3 reflects an increased adsorption capacity (q_o-mg g^{-1}) at elevated bed heights and initial metal ion concentrations for both raw and modified human hair. This might be because of the prevalence of more adsorption sites being available for metal ions as the height of the column is amplified. In contrast, the sorption capacity marked to drop with an increase in solution flow rate from 20 to 40 mL min^{-1}. At lesser solution flow rates, a prolonged interaction time among sorbent and metal ions directs to elevated rate constant values, signifying that the attainment of equilibrium with regard to adsorption capacity will be quite faster [37]. The rate constant K_{TH} marked a decrease with increased height and increased with a surge in solution flow rate as well as initial metal ion concentration. The R-squared value for the respective model (0.94–0.98) confirms the sound conformity among the observed and predicted values of the Thomas model, reflecting the suitability of the model where external as well as internal diffusion were not the rate-limiting steps [41].

3.2.2. Yoon-Nelson model

The highest 50 %-breakthrough time (τ) was marked at a bed height of 45 cm, following a decline with a decrease in bed height from 45 to 15 cm, owing it to the increased number of binding sites and a longer residence period at elevated bed heights [42]. Furthermore, K_{YN} declined with a rise in bed height for raw as well as modified human hair. This might be due to the probable reason that the elevated bed height stems from a prolonged service span for the breakthrough as well as the exhaustion period at a specified concentration. The τ reflected a profound dip at higher solution flow rates and initial metal ion concentrations, accounting for a lower abiding metal ion span in a fixed bed column [31]. R-square value in a range of 0.95–0.97 confirmed the applicability of the respective model to explain the experimental inferences.

3.2.3. Adam-Bohart model

The appraisal of model parameters reflected a decrease in N_o (maximum saturation capacity) and K_{AB} with an increase in bed height from 15 to 45 cm and an increase at elevated flow rates and initial metal ion concentration. This might be accredited to the prevalence of more adsorption sites at higher bed heights, leading to delayed maturation of fixed beds at elevated bed heights [43]. In addition, the increased N_o values at higher solution flow rates and initial metal ion concentration reflect that the approach was conquered by external mass transfer during the early phase of metal adsorption [44].

3.2.4. Bed Depth Service Time Model

The sorption capacity (N_o) and rate constant (K) were assessed at C_t/C_o equivalence of 0.1, 0.2, and 0.3 at different bed heights. The volumetric bed capacity (N_o) increased with the breakthrough, accounting for the enhanced interaction of metal ions with adsorbent molecules. In addition, it can be inferred that a lesser bed height, high solution flow rate, and influent metal ion concentration are prerequisites for earlier breakthroughs [45]. The correlation coefficient in the range of 0.97–0.99 suggests the apt suitability of the model to predict column adsorption performance.

3.3. Optimization of lead adsorption

The employment of Box-Behnken design was done for optimization of lead biosorption using fixed bed column. A total of seventeen experiments were devised, as portrayed in Table 1, to assess the effect of operational parameters encompassing bed height, solution flow rate, and initial metal ion concentration. Based on preliminary batch studies, the acid-modified human hair exhibited an edge over raw and bio-modified human hair with regard to lead adsorption. This inference is backed by the outcome of the breakthrough analysis depicted in Table 2 and Fig. 1. In view of this, only acid-modified human hair was subject to an optimization process with response surface methodology (RSM). The outcome of the RSM-based Box Behnken design reflected the empirical relationship of predicted response and operational variables as:

$$\begin{aligned}\textbf{Percent Removal} - \textbf{AMHH} = &+57.00362 + 0.608200\text{ bed height} + 0.594450\text{ flow rate} - 0.001750\text{ initial concentration}\\ &+ 0.0000202\text{ bed height} \times \text{bed height} - 0.011395\text{ flow rate} \times \text{flow rate} + 0.000410\text{ initial concentration}\\ &\times \text{initial concentration} - 0.007033\text{ bed height} \times \text{flow rate} - 0.001725\text{ bed height} \times \text{initial concentration}\\ &+ 0.000410\text{ flow rate} \times \text{initial concentration}\end{aligned}$$

The model was evaluated for its statistical quality using one-way ANOVA and Fischer's F-test. The ANOVA of lead adsorption by acid-modified human hair is illustrated in Table 4. The model generated for lead adsorption was significant, with an F-value of 40.14, illustrating that there is only a 0.01 % possibility that an F-value this huge might prevail because of noise. Exhibition of p-values <0.0500 signify the significant model terms. A, B, C, AB, AC, B^2 were significant model terms in the current model. Moreover, the Lack of Fit F-value was 2.01, reflecting a non-significant Lack of Fit compared to pure error. Conclusively, it can be inferred that bed height, solution flow rate, and initial metal ion concentration play their part in the adsorption of lead by acid-modified human hair.

The degree of fitting model for lead adsorption was appraised by R-squared value (Table-5). ANOVA results elucidate a high R-squared value of 0.98, which, in approximation to 1, reflects a substantial correlation between predicted and observed values. The acquired R^2 value suggests that the regression model successfully predicted and explained the association between the operating and the response variable. Specifically, the model accounted for 98 % of the overall variation in lead adsorption using acid-modified human hair, leaving only 2 % of residual variability for the respective model. The adjusted R-squared value measures how well the model accounts for the variability in the data, considering the complexity of the model. In contrast, the predicted R-squared value evaluates the model's accuracy in predicting the experimental response value [46]. The values pertaining to adjusted and predicted R^2 values are portrayed in Table 5 and signify a reasonable agreement between the two parameters as they exhibit a difference of less than 0.20 between them. Furthermore, the plot of experimental results (actual response) versus model results (predicted response) is exemplified in Fig. 2. The close alignment of the data points representing the percent removal and fit of percent removal suggests that the RSM-based Box Behnken model sufficiently captures and explains the range of experiments conducted. Similar dependence has been documented by Fawzy et al. [47] and Cardona et al. [23]. Moreover, the adequate precision quantifies the signal-to-noise proportion with a desirable mark of more or equal to 4. In the present study, a ratio of 22.784 designated an ample signal and suitability of the respective model to circumnavigate the design space. Perturbation plot aids in assessing the imprints of individual operational parameters on the response variable. A high slope parameter signifies the sensitivity towards response [48]. In the current study, the percent removal of lead ions reflects a high sensitivity in response to variations in bed height, solution flow rate, and initial metal ion concentration (Fig. 3).

3.4. *Effect of operational parameters and their interactions*

To address the impact of operational factors with their interactive imprints on lead adsorption efficiency, 2 d and 3 d surface plots were generated using design expert software and are illustrated in Figs. 4 and 5. These plots exist as a function of two operational variables while shelving the third operational parameter on hold. Fig. 4 (a) and 5 (a) present the interactive effect of bed height and solution flow rate. The response function (lead adsorption) was marked to increase from 72.95 to 82.16 % with escalation in bed height from 15 to 45 cm and declined from 72.95 to 69.39 with surge in flow rate from 20 to 40 mL min^{-1}. The increase in the percent removal of lead at elevated bed heights might be accredited to the expansion in the mass transfer zones at higher bed depths, while a low flow rate assists in improved interaction between sorbent and metal ions, directing to an augmented lead removal [49].

Fig. 4 (b) and 5 (b) represent the pooled Influence of bed height and initial metal ion concentration on the competence of lead adsorption. The solution flow rate was retained invariable to evaluate this interaction at 20 mL min^{-1}. The results inferred that with an increase in bed height from 15 to 45 cm and an increase in initial metal concentration from 60 to 140 mg L^{-1}, the adsorption increased from 70.09 to 80.25 %. This might be because of a longer mass transfer zone with increased bed heights, which creates a longer expanse for mass transfer zone to land at the column exit, thereby enhancing the metal uptake by an extended breakthrough time [50]. The increased adsorption of Pb lead ions with initial metal ion concentration might be because higher influent concentration furnished the transfer process a driving force to compensate for the mass transfer barrier [51].

The Influence of solution flow rate and influent metal concentration at a constant bed height of 45 cm is elucidated in Figs. 4(c) and 5(c). The percent removal of lead was marked maximum (79.39 %) at a flow rate of 20 ml min^{-1} and an initial metal ion concentration of 140 mg L^{-1}, while a minimum percent removal of 71.07 was observed at 20 mL min^{-1} flow rate and an initial metal ion concentration of 60 mg L^{-1}. When flow rates increase, the hindrance to mass transfer caused by the external film on the adsorbent surface is reduced. This results in a hastened mass transfer rate and a stunted enduring span. As a result, saturation is reached more quickly, leading to a decline in metal ions' removal efficiency [52]. The higher influent concentration of lead ions is directed to a higher driving force for the adsorption process, which leads to higher metal uptake and better column performance in the aftermath [53].

Table 4
Analysis of variance for RSM-based quadratic model for lead adsorption.

Source	Sum of Squares	df	Mean Square	F-value	p-value	
Model	196.44	9	21.83	40.14	<0.0001	significant
A-Bed Height	100.96	1	100.96	185.69	<0.0001	
B-Flow Rate	66.82	1	66.82	122.89	<0.0001	
C-Initial Conc.	12.95	1	12.95	23.82	0.0018	
AB	4.45	1	4.45	8.19	0.0243	
AC	4.28	1	4.28	7.88	0.0262	
BC	0.0081	1	0.0081	0.0149	0.9063	
A^2	0.0087	1	0.0087	0.0160	0.9028	
B^2	5.47	1	5.47	10.06	0.0157	
C^2	1.81	1	1.81	3.33	0.1109	
Residual	3.81	7	0.5437			
Lack of Fit	2.29	3	0.7624	2.01	0.2553	not significant
Pure Error	1.52	4	0.3797			
Cor Total	200.25	16				

Table 5
Model fit statistics.

	Per cent Removal
R^2	0.9810
Adjusted R^2	0.9566
Predicted R^2	0.8054
Adeq. Precision	22.7836

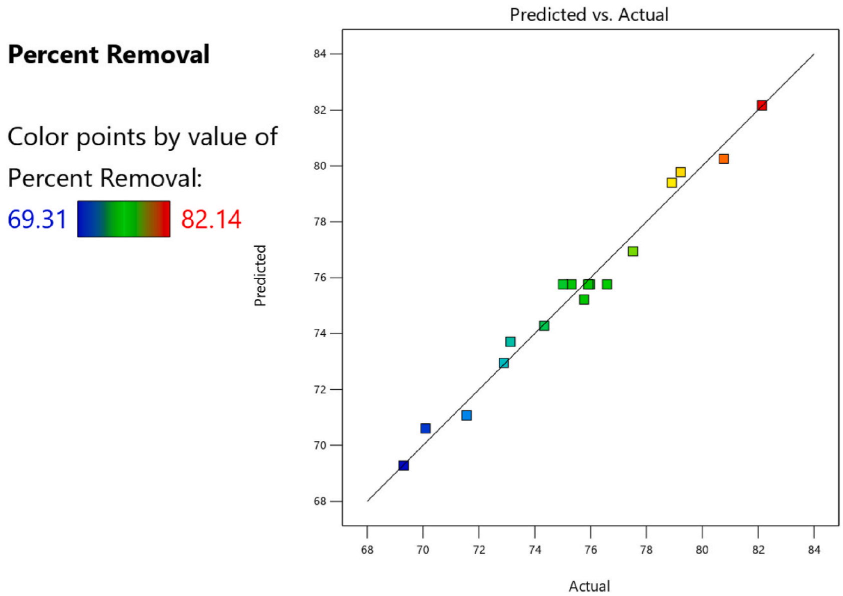

Fig. 2. Appraisal of experimental and predicted values for lead adsorption using acid-modified human hair.

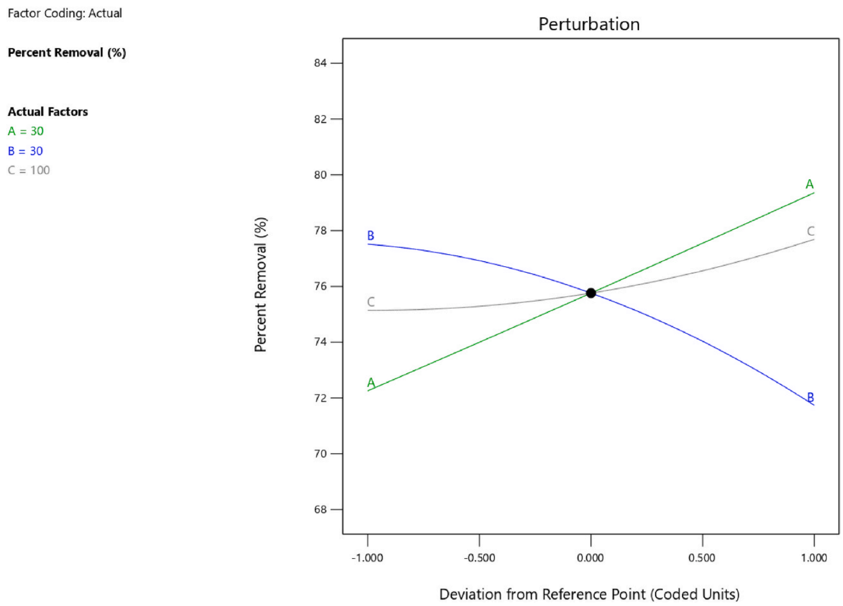

Fig. 3. Perturbation plot of lead adsorption by acid-modified human hair.

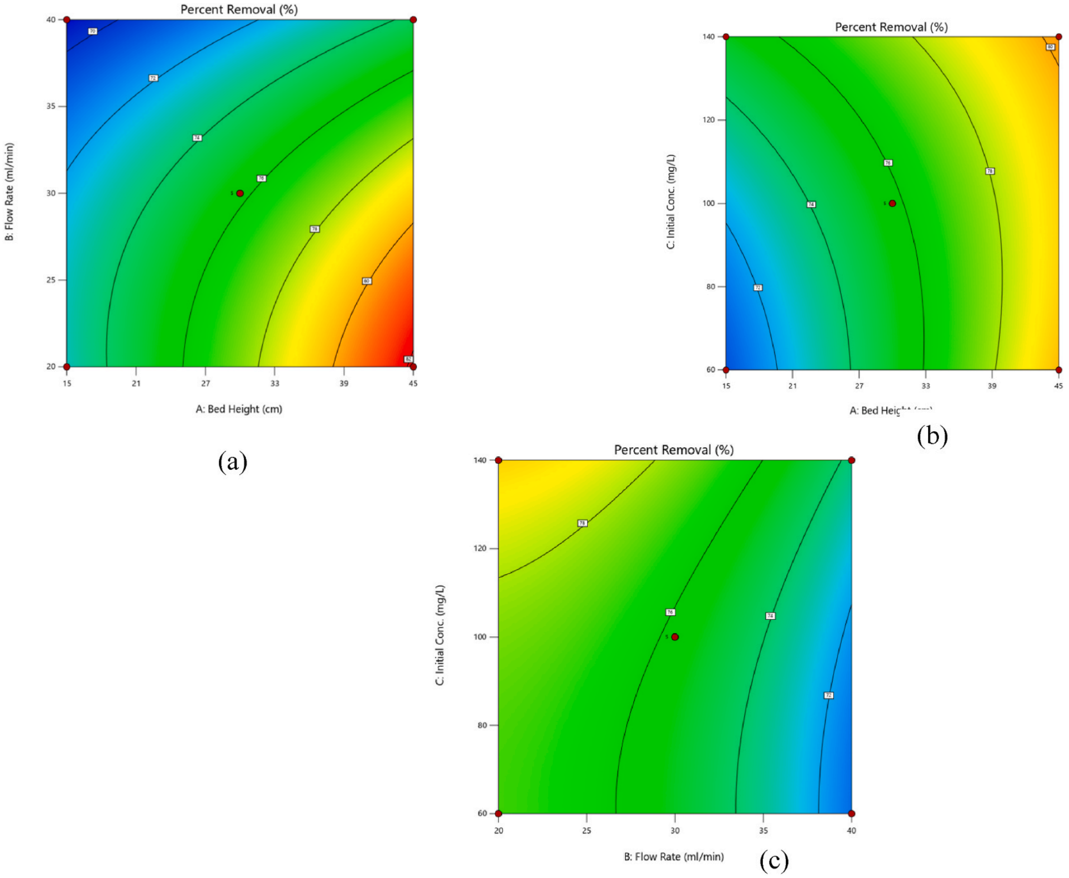

Fig. 4. 2D-response surface plots to appraise the Influence of (a) bed height and flow rate (b) bed height and initial concentration (c) flow rate and initial concentration on lead adsorption by acid modified Human Hair.

3.5. *Optimization of lead adsorption*

The present investigation exploited the numerical optimization of RSM to optimize lead adsorption. The optimization of response serves researchers to arrive at an anticipated goal within the defined range of factors and determine operational parameters that ensure this desirable response. One hundred solutions with different combinations of operational variables were deduced. However, the optimal conditions for achieving a solution with high desirability (1.00) were determined to be a bed height of 42.79 cm, a solution flow rate of 20.92 mL $min^{-1,}$ and an initial metal concentration of 139.51 mg L^{-1} (Figure-6). Under these optimized conditions, the percentage of lead removal using acid-modified human hair was 82.31 %. The experimental results performed under these optimized conditions approximately revealed a percent removal of 85.05 %, reflecting reasonable conformity with values acquired through the Box-Behnken design. The contour plots elucidating the desirability and corresponding percent removal under optimized operating conditions are illustrated in Fig. 7.

3.6. *Mechanism of adsorption*

Human hair comprises of various tiny cracks on the surface which account for physical adsorption of metal ions onto human hair. In addition, human hair consists of long peptide chains containing unshared pair of electrons in atoms such a nitrogen and oxygen. These atoms facilitate the binding of heavy metals via chemical adsorption [54]. Moreover, human hair entails a high proportion of sulfur-containing cysteine amino acids, which strongly coordinate to heavy metal ions, thereby strengthening the chemical adsorption onto the hair [15]. The higher adsorption of lead ions by acid-modified human hair might be due to the reduction of sulfide bonds to mercapo groups, which facilitate the coordination of heavy metal ions. The mechanism is illustrated in Fig. 8. Similar dependnece has been put forward by Roh et al. [29].

3.7. *Regeneration of spent adsorbents*

The recovery of adsorbed metal ions and re-use of adsorbents is of considerable importance from the perspective of practical

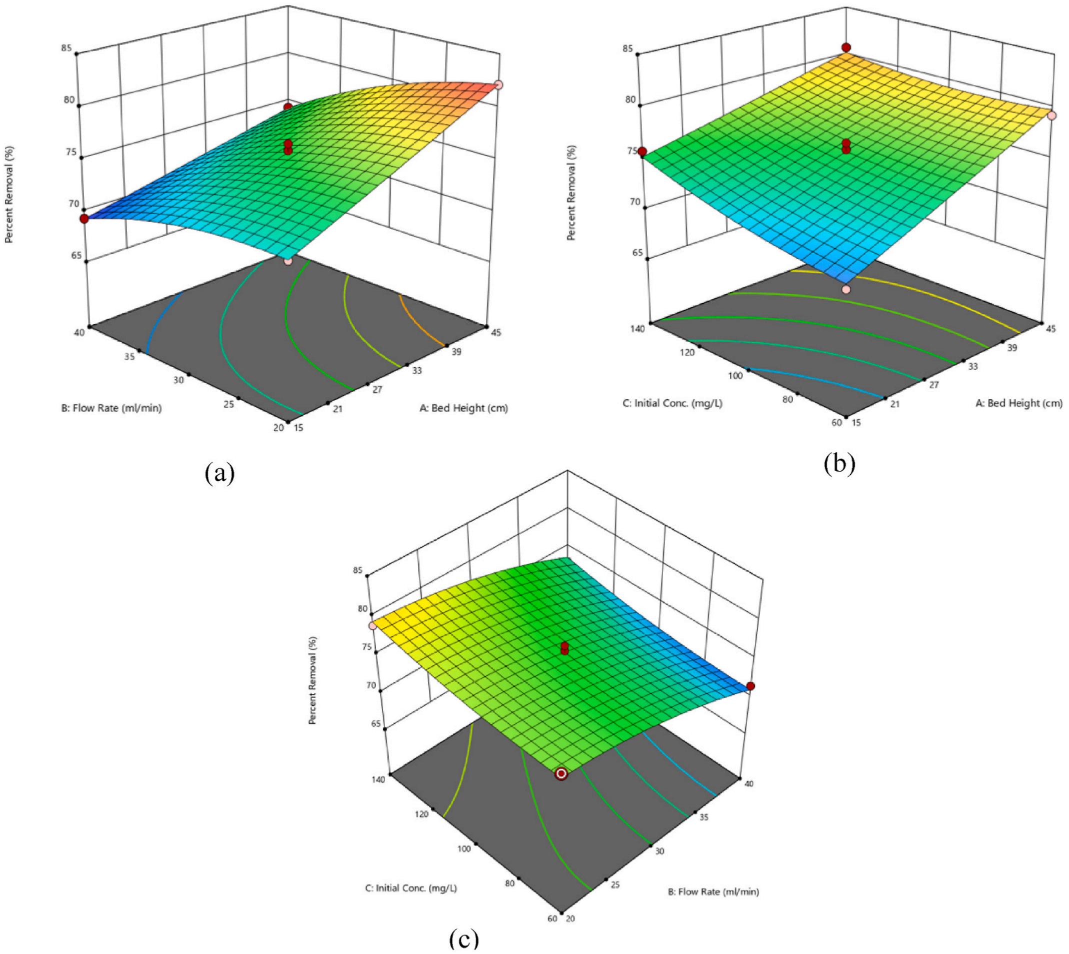

Fig. 5. 3D-response surface plots to appraise the Influence of (a) bed height and flow rate, (b) bed height and initial concentration, (c) flow rate and initial concentration on lead adsorption by acid modified Human Hair.

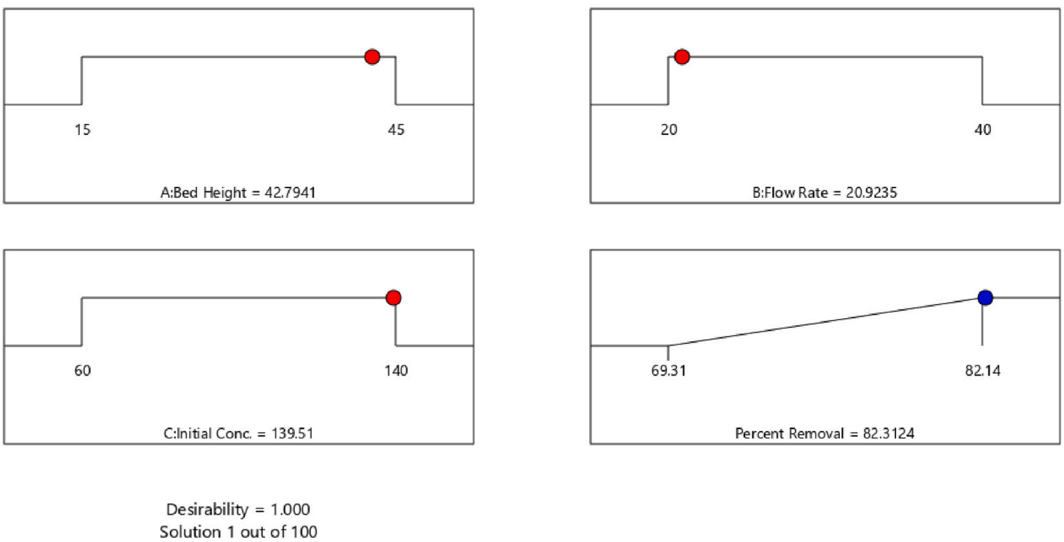

Fig. 6. Optimization of lead adsorption in a fixed-bed column using acid modified Human Hair.

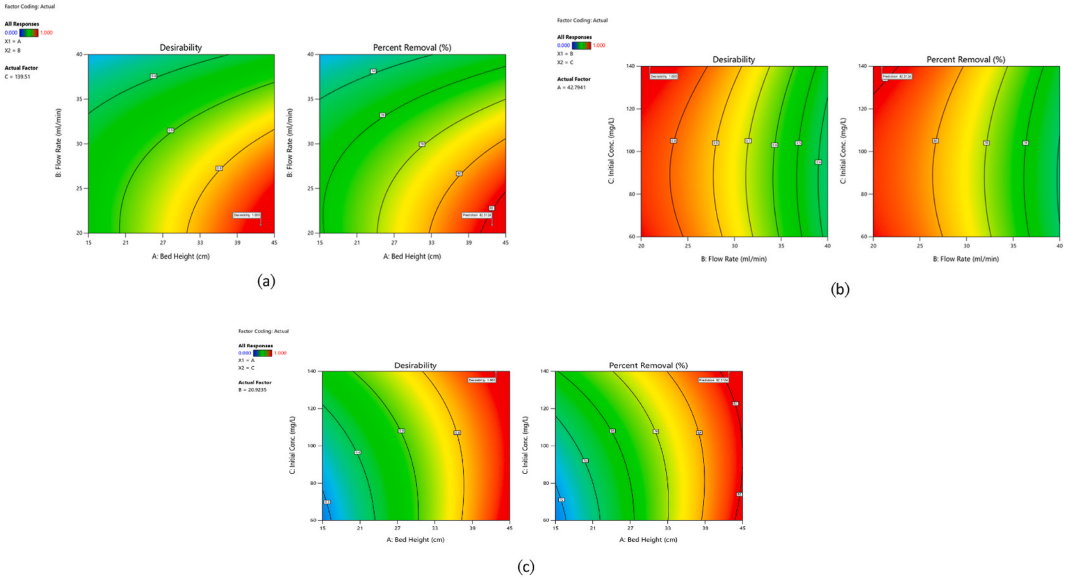

Fig. 7. 2D contour plots elucidating the desirability and corresponding percent removal under optimized operating conditions (a) Bed height and Flow rate (b) Flow rate and Initial metal ion concentration (c) Bed height and Initial metal ion concentration.

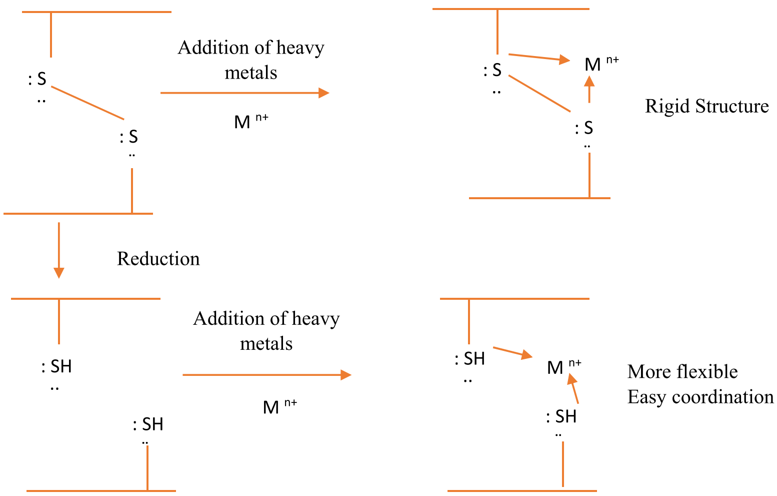

Fig. 8. Removal of metal ions with reduced human hair.

application. The regeneration of adsorbents is acknowledged for deducing the operational cost substantially [55]. The spent adsorbents were regenerated and reused for lead adsorption at a bed height of 45 cm, a solution flow rate of 20 ml min^{-1}, and an initial metal concentration of 140 mg L^{-1}. The comparative adsorption efficiencies of fresh and regenerated adsorbents using raw and modified human hair is illustrated in Fig. 9. The adsorption efficiency of raw, acid-modified, and bio-modified human hair for lead ions decreased from 81.01 to 48.84 %, 85.05 to 51.84 %, and 83.87 to 50.02 %, respectively, after three adsorption-desorption cycles. These observations reflect that the raw and modified rice straw could be reutilized to remove lead ions for three adsorption-desorption cycles, illustrating the economic feasibility and commercial applicability of the absorbent. EDTA integrates the acidic and complexing effect to liberate adsorbed lead ions on the adsorbent surface. The substantial elution of lead ions with EDTA solution allow their use for subsequent adsorption cycle or the eluted adsorbents can be employed for the reinforcement of construction materials [56].

3.8. Comparison with other related studies

The observations acquired in the current study were compared with other related investigations and the results are presented in Table 6. The current adsorbents possessed a competitive performance with other adsorbents for metal adsorption. Undoubtedly, activated carbon exhibits high efficiency in removing lead ions but the practicability of activated carbon remains a drawback, despite

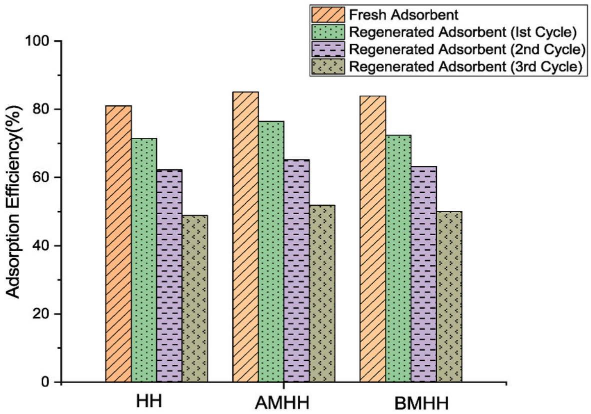

Fig. 9. Adsorption efficiency of fresh and regenerated adsorbents- HH: Human Hair, AMHH: Acid-Modified Human Hair, BMHH: Bio-Modified Human Hair for lead adsorption across three adsorption-desorption cycles.

Table 6
Comparison of lead adsorption capacities with other adsorbents.

Adsorbent	Adsorption Capacities q_{max}(mg g^{-1})	References
Olive stone	6.39	Blázquez et al. [58]
Rice husk	21.38	Singha and Das [59]
Walnut Shell	3.59	Das et al. [55]
Almond Shell	3.58	Das et al. [55]
NaOH-rice husk ash spirogyra	1.33	Yahya et al. [35]
Surgarcane baggase	0.143	Vera et al. [60]
Sago Bark	22.26	Fauzia et al. [61]
Ficus benghalenesis leaf powder	12.27	Hymavathi and Prabhakar [62]
Ni-Alginate Hydrogel Beads	15.70	Sami et al. [63]
Commercial Activated Carbon	45.82	Hameed et al. [64]
Rosa damascena waste	24.90	Batool et al. [65]
Human Hair	1.75	Preseent study
Acid-Modified Human Hair	1.79	Preseent study
Bio-Modified Human Hair	1.77	Preseent study

its widespread use [57]. In addition, activated carbon is comparatively expensive and is difficult to recycle because of the strong interaction between activated carbon and heavy metal ions [17]. The adsorbents employed in the current study are renewable and cost-effective, delivering additional benefits regarding their applicability in water treatment. The employment of human hair as a low-cost adsorbent was considered due to its high stability, ready accessibility, and ubiquitous nature, the accumulation of which would cause serious environmental concerns. Therefore, the advantage of this waste as a new raw material is of interest and pays to the idea of circular economy.

4. Conclusion

The acquired observations elucidated that for raw and modified adsorbents, the breakthrough time was higher at elevated bed height, low initial metal ion concentration, and low solution flow rate. Among the employed models, Bed Depth Service Time (BDST) and the Thomas model exhibited the highest R-squared value for most cases. The developed polynomial quadratic models for lead adsorption with acid-modified human hair validated a strong confirmation with the experimental data at a 95 % significance level. This was evident from the high regression parameters obtained ($R^2 = 0.98$), and further validation was confirmed through analysis of variance (ANOVA), affirming the cogency of the proposed model. The optimal conditions (desirability-1.00) for achieving a goal of maximum percent removal of lead ions were marked to be a bed height of 42.79 cm, solution flow rate of 20.92 mL $min^{-1,}$ and an initial metal concentration of 139.51 mg L^{-1}. The percent removal of lead under these optimized conditions reflected a reasonable conformity with values acquired through the Box-Behnken design. Conclusively, it can be inferred from the results that modified human hair offers an appealing adsorbent for the remediation of lead (Pb) ions from aqueous solution, thus reinforcing the concept of waste to wealth. In addition, the RSM-based Box-Behnken mirrors a proficient and consistent means to appraise and optimize the operational parameters regarding heavy metal adsorption in a fixed-bed column.

Funding

This research was funded by the National Key R&D Program of China (2021YDF1700900).

Data availability statement

All data included in article/supp. material/referenced in article.

CRediT authorship contribution statement

Aanisa Manzoor Shah: Writing – original draft, Resources, Methodology, Investigation, Formal analysis, Data curation, Conceptualization. **Inayat Mustafa Khan:** Writing – review & editing, Visualization, Software, Formal analysis. **Zhenjie Du:** Visualization, Validation, Project administration, Funding acquisition, Data curation. **Rehana Rasool:** Methodology, Formal analysis, Data curation. **Raihana Habib Kant:** Writing – review & editing, Visualization, Validation, Software, Investigation. **Shakeel Mir:** Writing – review & editing, Investigation, Formal analysis, Data curation. **Tahir A. Sheikh:** Writing – review & editing, Visualization, Validation, Investigation, Formal analysis. **Fehim Jeelani Wani:** Writing – review & editing, Visualization, Validation, Software, Formal analysis. **M. Ayoub Bhat:** Validation, Methodology, Investigation, Formal analysis. **Javid A. Bhat:** Writing – review & editing, Visualization, Validation, Software, Methodology. **M.H. Chesti:** Writing – review & editing, Software, Formal analysis, Data curation. **Mumtaz A. Ganie:** Writing – review & editing, Validation, Software, Methodology, Formal analysis. **Yasir Hanif Mir:** Visualization, Validation, Software, Methodology, Formal analysis. **Tsering Dolker:** Visualization, Validation, Software, Methodology, Investigation. **Sulaiman Ali Alharbi:** Writing – review & editing, Visualization, Validation, Resources, Funding acquisition. **Tahani Awad Alahmadi:** Writing – review & editing, Visualization, Validation, Resources, Funding acquisition. **Shafeeq Ur Rahman:** Writing – original draft, Visualization, Supervision, Project administration, Funding acquisition.

Declaration of competing interest

The authors declare that they have no known competing financial interests or personal relationships that could have appeared to influence the work reported in this paper.

Acknowledgement

This project was supported by Researchers Supporting Project Number (RSP2025R230) King Saud University, Riyadh, Saudi Arabia.

References

[1] A. Boretti, L. Rosa, Reassessing the projections of the world water development report, NPJ Clean Water 2 (1) (2019) 15.
[2] E.J.O. Godwin, V. Chandrasekaran, A.C. Smah, E.O. Faith, Emerging infectious food system related zoonotic foodborne disease–A threat to global food safety and nutrition security, in: Foodborne Pathogens-Recent Advances in Control and Detection, IntechOpen, 2022.
[3] R. Connor, et al., T. He United Nations World Water Development Report 2017. Wastewater: the Untapped Resource, The United Nations World Water Development Report (United Nations Educational, Scientific and Cultural Organization, New York, United States, 2017.
[4] G. Ryder, The United Nations World Water Development Report, 2017: Wastewater: the Untapped Resource, 2017.
[5] A.K. Islam, Domestic and industrial wastewater generation and its energy recovery potential in Bangladesh, Cleaner Energy Systems 6 (2023) 100092.
[6] B. Singha, N. Bar, S.K. Das, The use of artificial neural network (ANN) for modeling of Pb (II) adsorption in batch process, J. Mol. Liq. 211 (2015) 228–232.
[7] G.K. Kinuthia, V. Ngure, D. Beti, R. Lugalia, A. Wangila, L. Kamau, Levels of heavy metals in wastewater and soil samples from open drainage channels in Nairobi, Kenya: community health implication, Sci. Rep. 10 (1) (2020) 8434.
[8] T. Mitra, B. Singha, N. Bar, S.K. Das, Removal of Pb (II) ions from aqueous solution using water hyacinth root by fixed-bed column and ANN modeling, J. Hazard Mater. 273 (2014) 94–103.
[9] A. Mirzaei, A. Ebadi, P. Khajavi, Kinetic and equilibrium modeling of single and binary adsorption of methyl tert-butyl ether (MTBE) and tert-butyl alcohol (TBA) onto nano-perfluorooctyl alumina, Chem. Eng. J. 231 (2013) 550–560.
[10] A.A. Mohammed, O.A. Abdel Moamen, S.S. Metwally, A.M. El-Kamash, I. Ashour, M.S. Al-Geundi, Utilization of modified attapulgite for the removal of Sr (II), Co (II), and Ni (II) ions from multicomponent system, part I: kinetic studies, Environ. Sci. Pollut. Control Ser. 27 (2020) 6824–6836.
[11] E. Bazrafshan, L. Mohammadi, A. Ansari-Moghaddam, A.H. Mahvi, Heavy metals removal from aqueous environments by electrocoagulation process–a systematic review, Journal of environmental health science and engineering 13 (2015) 1–16.
[12] M.M. Kabir, M.M. Akter, S. Khandaker, B.H. Gilroyed, M. Didar-ul-Alam, M. Hakim, M.R. Awual, Highly effective agro-waste based functional green adsorbents for toxic chromium (VI) ion removal from wastewater, J. Mol. Liq. 347 (2022) 118327.
[13] I. Zahara, M. Arshad, M.A. Naeth, T. Siddique, A. Ullah, Feather keratin derived sorbents for the treatment of wastewater produced during energy generation processes, Chemosphere 273 (2021) 128545.
[14] H. Zhang, F. Carrillo, M. López-Mesas, C. Palet, Valorization of keratin biofibers for removing heavy metals from aqueous solutions, Textil. Res. J. 89 (7) (2019) 1153–1165.
[15] C.T. Low, Human Hair Keratin and its Interaction with Metal Ions, 2020.
[16] A. Rigo, A. Corazza, M.L. di Paolo, M. Rossetto, R. Ugolini, M. Scarpa, Interaction of copper with cysteine: stability of cuprous complexes and catalytic role of cupric ions in anaerobic thiol oxidation, J. Inorg. Biochem. 98 (9) (2004) 1495–1501.
[17] H. Zhang, F. Carrillo-Navarrete, M. López-Mesas, C. Palet, Use of chemically treated human hair wastes for the Removal of heavy metal ions from water, Water 12 (5) (2020) 1263.
[18] Z. Khoshraftar, H. Masoumi, A. Ghaemi, Experimental, response surface methodology (RSM) and mass transfer modeling of heavy metals elimination using dolomite powder as an economical adsorbent, Case Studies in Chemical and Environmental Engineering 7 (2023) 100329.
[19] M.I. Khalil, Co-precipitation in aqueous solution synthesis of magnetite nanoparticles using iron (III) salts as precursors, Arab. J. Chem. 8 (2) (2015) 279–284.
[20] H. Pashaei, A. Ghaemi, M. Nasiri, B. Karami, Experimental modeling and optimization of CO2 absorption into piperazine solutions using RSM-CCD methodology, ACS Omega 5 (15) (2020) 8432–8448.
[21] R. Sasidharan, A. Kumar, Response surface methodology for optimization of heavy metal removal by magnetic biosorbent made from anaerobic sludge, J. Indian Chem. Soc. 99 (9) (2022) 100638.
[22] M.O. Borna, M. Pirsaheb, M.V. Niri, R.K. Mashizie, B. Kakavandi, M.R. Zare, A. Asadi, Batch and column studies for the adsorption of chromium (VI) on low-cost Hibiscus Cannabinus kenaf, a green adsorbent, J. Taiwan Inst. Chem. Eng. 68 (2016) 80–89.

[23] Y. Cardona, S.A. Korili, A. Gil, Use of response surface methodology to optimize triclosan adsorption on alumina pillared clays in a fixed-bed column for applications in solid-phase extraction, Appl. Clay Sci. 235 (2023) 106879.
[24] M. Calero, A. Ronda, A. Pérez, A. Yáñez, M.C. Trujillo, M.Á. Martín-Lara, The scale-up of Cr3+ biosorption onto olive stone in a fixed bed column, Desalination Water Treat. 57 (52) (2016) 25140–25152.
[25] A. Ghribi, M. Chlendi, Modeling of fixed bed adsorption: application to the adsorption of an organic dye, Asian J. Textil. 1 (4) (2011) 161–171.
[26] H.A. Rojas, D.C. Guerrero, O.Y. Vásquez, J.S. Valencia, Aplicación del modelo de Bohart y Adams en la remoción de mercurio de drenajes de minería por adsorción con carbón activado, Inf. Tecnol. 23 (3) (2012) 21–32.
[27] M.A.M. Altufaily, N.J. Al-Mansori, A.F.M. Al-Qaraghulee, Mathematical modeling of fixed-bed columns for the adsorption of methylene blue on to fired clay pot, Int. J. ChemTech Res. 12 (2019) 70–80.
[28] W. Somyanonthanakun, R. Ahmed, V. Krongtong, S. Thongmee, Studies on the adsorption of Pb (II) from aqueous solutions using sugarcane bagasse-based modified activated carbon with nitric acid: kinetic, isotherm and desorption, Chemical Physics Impact 6 (2023) 100181.
[29] H.G. Roh, S.G. Kim, J. Jung, Adsorption of heavy-metal ions (Pb^{2+}, Cu^{2+}) on perm-lotion-treated human hair, Kor. J. Chem. Eng. 31 (2014) 310–314.
[30] T. Mitra, N. Bar, S.K. Das, Rice husk: green adsorbent for Pb (II) and Cr (VI) removal from aqueous solution—column study and GA–NN modeling, SN Appl. Sci. 1 (2019) 1–15.
[31] S.E. Marrane, K. Dânoun, Y. Essamlali, S. Aboulhrouz, S. Sair, O. Amadine, M. Zahouily, Fixed-bed adsorption of Pb (ii) and Cu (ii) from multi-metal aqueous systems onto cellulose-g-hydroxyapatite granules: optimization using response surface methodology, RSC Adv. 13 (45) (2023) 31935–31947.
[32] H.A. Ibrahim, S.S. Metwally, W.R. Mohamed, E.A. El-Sherief, H.S. Mekhamer, I.M. Moustafa, E.M. Mabrouk, Performance evaluation of fixed bed column packed with ionic liquid impregnated silica for separation of gadolinium and neodymium from aqueous solutions, Chromatographia 84 (2021) 335–345.
[33] M. Imran, M.M. Iqbal, J. Iqbal, N.S. Shah, Z.U.H. Khan, B. Murtaza, M. Rizwan, Synthesis, characterization and application of novel MnO and CuO impregnated biochar composites to sequester arsenic (As) from water: modeling, thermodynamics and reusability, J. Hazard Mater. 401 (2021) 123338.
[34] G.M. Shah, M. Imran, U. Aiman, M.M. Iqbal, M. Akram, H.M.R. Javeed, F. Rabbani, Efficient sequestration of lead from aqueous systems by peanut shells and compost: evidence from fixed bed column and batch scale studies, PeerJ Physical Chemistry 4 (2022) e21.
[35] M.D. Yahya, H. Abubakar, K.S. Obayomi, Y.A. Iyaka, B. Suleiman, Simultaneous and continuous biosorption of Cr and Cu (II) ions from industrial tannery effluent using almond shell in a fixed bed column, Results in Engineering 6 (2020) 100113.
[36] M.D. Yahya, J.O. Odigure, Fixed bed column study for Pb(II) adsorption using calcium-alginate Shea butter husk (TSBH), in: 5th International Conference on Industrial Engineering and Operations Management, 2015.
[37] A.H. Alamin, L. Kaewsichan, Adsorption of Pb (II) Ions from aqueous solution in fixed bed column by mixture of clay plus bamboo biochar, Walailak J. Sci. Technol. 13 (11) (2016) 949–963.
[38] S. Mnasri-Ghnimi, N. Frini-Srasra, Removal of heavy metals from aqueous solutions by adsorption using single and mixed pillared clays, Appl. Clay Sci. 179 (2019) 105151.
[39] V.K.C. Lee, J.F. Porter, G. McKay, Development of fixed-bed adsorber correlation models, Ind. Eng. Chem. Res. 39 (2000) 2427–2433.
[40] H. Patel, Batch and continuous fixed bed adsorption of heavy metals removal using activated charcoal from neem (azadirachta indica) leaf powder, Sci. Rep. 10 (2020) 16895.
[41] S.S. Baral, N. Das, T.S. Ramulu, S.K. Sahoo, S.N. Das, G.R. Chaudhury, Removal of Cr (VI) by thermally activated weed Salvinia cucullata in a fixed-bed column, J. Hazard Mater. 161 (2–3) (2009) 1427–1435.
[42] S.S. Metwally, H.S. Mekhamer, E.A. El-Sherief, Encapsulation of nano-sized iron (III)–titanium (IV) mixed oxide for the removal of Co (II), Cd (II) and Ni (II) ions using continuous-flow column: multicomponent Solution, Separ. Sci. Technol. 55 (11) (2020) 1932–1946.
[43] A.P. Lim, A.Z. Aris, Continuous fixed-bed column study and adsorption modeling: removal of cadmium (II) and lead (II) ions in aqueous solution by dead calcareous skeletons, Biochem. Eng. J. 87 (2014) 50–61.
[44] R. Han, L. Zou, X. Zhao, Y. Xu, F. Xu, Y. Li, Y. Wang, Characterization and properties of iron oxide-coated zeolite as adsorbent for Removal of copper (II) from solution in fixed bed column, Chem. Eng. J. 149 (1–3) (2009) 123–131.
[45] R.V. Saravanan, R. Yuvaraja, L. Andal, V. Yogeshwaran, Evaluation of the performance of packed bed column for heavy metal ion removal using rice husk powder coated with iron oxide nano-particles, GLOBAL NEST JOURNAL 24 (3) (2022) 474–486.
[46] W.T. Tee, N.Y.L. Loh, B.Y.Z. Hiew, S. Hanson, S. Thangalazhy-Gopakumar, S. Gan, L.Y. Lee, Effective remediation of lead (II) wastewater by Parkia speciosa pod biosorption: Box-Behnken design optimisation and adsorption performance evaluation, Biochem. Eng. J. 187 (2022) 108629.
[47] M.A. Fawzy, H. Darwish, S. Alharthi, M.I. Al-Zaban, A. Noureldeen, S.H. Hassan, Process optimization and modeling of Cd2+ biosorption onto the free and immobilized Turbinaria ornata using Box–Behnken experimental design, Sci. Rep. 12 (1) (2022) 3256.
[48] G.M. Sawood, S.B. Gautam, A. Mishra, S. Dixit, N. Singh, Modeling of the as (III) adsorption using Fe impregnated polyethylene terephthalate char matrix: a statistical approach, Water Sci. Technol. 86 (7) (2022) 1790–1809.
[49] I.K. Rind, N. Memon, M.Y. Khuhawar, W.A. Soomro, M.F. Lanjwani, Modeling of cadmium (II) removal in a fixed bed column utilizing hydrochar-derived activated carbon obtained from discarded mango peels, Sci. Rep. 12 (1) (2022) 8001.
[50] Z.Z. Chowdhury, S.M. Zain, R.A. Khan, R.F. Rafique, K. Khalid, Batch and fixed bed adsorption studies of lead (II) cations from aqueous solutions onto granular activated carbon derived from Mangostana garcinia shell, Bioresources 7 (3) (2012) 2895–2915.
[51] C. Phawachalotorn, W. Wongniramaikul, T. Taweekarn, B. Kleangklao, W. Pisitaro, W. Limsakul, A. Choodum, Continuous phosphate removal and recovery using a calcium silicate hydrate composite monolithic cryogel column, Polymers 15 (3) (2023) 539.
[52] M.A.E. de Franco, C.B. de Carvalho, M.M. Bonetto, R. de Pelegrini Soares, L.A. Féris, Diclofenac removal from water by adsorption using activated carbon in batch mode and fixed-bed column: isotherms, thermodynamic study and breakthrough curves modeling, J. Clean. Prod. 181 (2018) 145–154.
[53] M.H. Marzbali, M. Esmaieli, Fixed bed adsorption of tetracycline on a mesoporous activated carbon: experimental study and neuro-fuzzy modeling, J. Appl. Res. Technol. 15 (5) (2017) 454–463.
[54] F. Ogata, N. Nagai, A. Soeda, K. Yamashiro, T. Nakamura, C. Saenjum, N. Kawasaki, Removal of Sr (II) ions from aqueous solution by human hair treated with EDTA, Bioresour. Technol. Rep. 9 (2020) 100393.
[55] A. Das, N. Bar, S.K. Das, Pb (II) adsorption from aqueous solution by nutshells, green adsorbent: adsorption studies, regeneration studies, scale-up design, its effect on biological indicator and MLR modeling, J. Colloid Interface Sci. 580 (2020) 245–255.
[56] K.K. Mondal, S. Banerjee, S. Dhar, M. Sudarshan, P. Bhattacharjee, The impact of human waste hair reprocessing occupation on environmental degradation—a case study from rural West Bengal, India, Environ. Geochem. Health 42 (10) (2020) 3157–3170.
[57] A.K. Tolkou, K.N. Maroulas, D. Theologis, I.A. Katsoyiannis, G.Z. Kyzas, Comparison of Modified Peels: Natural Peels or Peels-Based Activated Carbons for the Removal of Several Pollutants Found in Wastewaters 10 (1) (2024) 22. C.
[58] G. Blázquez, M. Calero, F. Hernáinz, G. Tenorio, M.A. Martín-Lara, Equilibrium biosorption of lead (II) from aqueous solutions by solid waste from olive-oil production, Chem. Eng. J. 160 (2) (2010) 615–622.
[59] B. Singha, S.K. Das, Removal of Pb (II) ions from aqueous solution and industrial effluent using natural biosorbents, Environ. Sci. Pollut. Control Ser. 19 (2012) 2212–2226.
[60] L.M. Vera, D. Bermejo, M.F. Uguña, N. Garcia, M. Flores, E. González, Fixed bed column modeling of lead (II) and cadmium (II) ions biosorption on sugarcane bagasse, Environmental Engineering Research 24 (1) (2019) 31–37.
[61] S. Fauzia, H. Aziz, D. Dahlan, R. Zein, Modelling for removal of Cr (VI) and Pb (II) using sago bark (Metroxylon sagu) by fixed-bed column method, Egypt. J. Chem. 64 (8) (2021) 3981–3989.
[62] D. Hymavathi, G. Prabhakar, Modeling of cobalt and lead adsorption by Ficus benghalenesis L. in a fixed bed column, Chem. Eng. Commun. 206 (10) (2019) 1264–1272.

[63] N.M. Sami, A.A. Elsayed, M.M.S. Ali, S.S. Metwally, Ni-alginate hydrogel beads for establishing breakthrough curves of lead ions removal from aqueous solutions, Environ. Sci. Pollut. Control Ser. 29 (53) (2022) 80716–80726.
[64] A. Hameed, B.H. Hameed, F.A. Almomani, M. Usman, M.M. Ba-Abbad, M. Khraisheh, Dynamic simulation of lead (II) metal adsorption from water on activated carbons in a packed-bed column, Biomass Conversion and Biorefinery (2022) 1–10.
[65] F. Batool, T.A. Kurniawan, A. Mohyuddin, M.H.D. Othman, I. Ali, G. AbdulKareem-Alsultan, K.W. Chew, Rosa damascena waste as biosorbent for co-existing pollutants removal: fixed-bed column study and ANN modeling, Chem. Eng. Sci. 293 (2024) 120057.